Biota: Jurnal Ilmiah Ilmu-Ilmu Hayati, Vol. 11(3): 405-418, Oktober 2026
p-ISSN 2527-3221, e-ISSN 2527-323X, https://ojs.uajy.ac.id/index.php/biota/issue/view/585
DOI: 10.24002/biota.v11i3.12790

Galangal Rhizomes Phytoconstituents as VEGFR2 Inhibitors in Breast Cancer: Computational studies

Keisya Ghaliyah Purnomo[1], Gabriel Daendya Amalia Bintang Christy[1], Jahraema Deagustia Ningsih[1], Jihan Sadira Aurellia[1], Dhania Novitasari[2*]

[1]Undergraduate Pharmacy Study Program Department of Pharmaceutical Analysis and Medicinal Chemistry, Faculty of Pharmacy, Padjadjaran University
Jl. Sumedang, West Java, Indonesia
[2]Department of Pharmaceutical Analysis and Medicinal Chemistry, Faculty of Pharmacy, Padjadjaran University
Jl. Sumedang, West Java, Indonesia
Email: dhania@unpad.ac.id **Corresponding Author*

Abstract

Breast cancer is the most frequently diagnosed cancer and the leading cause of cancer death among women in Indonesia. Vascular endothelial growth factor receptor 2 (VEGFR-2), a key regulator of tumour angiogenesis, is an established therapeutic target, but existing inhibitors are costly and poorly tolerated. This study evaluated ten compounds reported from *Kaempferia galanga* rhizomes as potential VEGFR-2 inhibitors using in silico approaches, including Lipinski's Rule of Five, ADMET prediction with PreADMET, pharmacophore screening with LigandScout, and molecular docking against VEGFR-2 (PDB ID: 3VO3). All ten compounds satisfied the Rule of Five. The selected pharmacophore model (Model 4, AUC = 0.78) retrieved eight of them as hits. Redocking of the native imidazo[1,2-b]pyridazine ligand gave an RMSD of 1.29 Å, a binding energy of -10.81 kcal/mol and a Ki of 11.93 nM, validating the protocol. Sandaracopimaradien-6β,9α-diol-1-one gave the lowest binding energy among the test compounds (-9.23 kcal/mol; Ki 172.53 nM) but formed no hydrogen bonds and failed the pharmacophore filter. Seven phenolic compounds reproduced the native ligand's hydrogen bond to Glu885. Taking drug-likeness, predicted toxicity, pharmacophore fit and binding mode together, methyl (2R,3S)-2,3-dihydroxy-3-(4-methoxyphenyl)propanoate was the most promising VEGFR-2 inhibitor candidate, and confirmation by in vitro and in vivo testing is required.

Keywords: Breast cancer, Galangal, Molecular docking, In silico, VEGFR2

Submitted: 10 September 2025; Revised: 24 October 2026; Accepted: 27 October 2026

Introduction

Breast cancer is a malignant tumour that originates in breast tissue, arising from either the lobular components or the ductal epithelium. It develops when cells lose control over normal division, leading to abnormal, rapid and uncontrolled growth (Rizka et al., 2022). These abnormal cells continue to divide and form a lump in the breast, which can ultimately prove fatal (Satriyo et al., 2018). Breast cancer was chosen as the focus of this study for three reasons. First, it is the most frequently diagnosed cancer in women worldwide: GLOBOCAN recorded approximately 2.3 million new cases and 685,000 deaths in 2020, making it the leading cause of cancer death among women (Ghoncheh et al., 2016; Sung et al., 2021). Second, Indonesia carries a disproportionate share of that burden, with 65,858 new breast cancer cases reported annually against a national cancer prevalence of 1,017,290 cases in RISKESDAS 2018, and breast cancer has the highest prevalence of any cancer among Indonesian women (Mboi et al., 2022). Third, and most relevant here, breast tumours depend heavily on angiogenesis for growth and metastasis, and VEGFR-2 expression in breast

Copyright© 2026. Keisya Ghaliyah Purnomo, Gabriel Daendya Amalia Bintang Christy, Jahraema Deagustia Ningsih, Jihan Sadira Aurellia, Dhania Novitasari

This work is licensed under a Creative Commons Attribution-NonCommercial 4.0 International License

How to Cite: Purnomo, K. G., Christy, G. D. A. B., Ningsih, J. D., Aurellia, J. S., & Novitasari, D. (2026). Galangal Rhizomes Phytoconstituents as VEGFR2 Inhibitors in Breast Cancer: Computational studies. Biota: Jurnal Ilmiah Ilmu-Ilmu Hayati, 11(3),405-418.

tissue is closely linked both to disease progression and to resistance to endocrine therapy (Luo et al., 2017; Zhu & Zhou, 2015). Breast cancer therefore provides a clearer mechanistic rationale for targeting VEGFR-2 than tumour types in which angiogenic signalling is less central.

Vascular endothelial growth factor (VEGF) is a 40-45 kDa homodimeric protein secreted by various cells under both physiological and pathological conditions (Patel et al., 2023). Vascular endothelial growth factor-A (VEGF-A) is the primary factor regulating endothelial cell function in vasculogenesis and angiogenesis. VEGF consists of five members: VEGF-A, VEGF-B, VEGF-C, VEGF-D, and placenta growth factor. As a ligand, VEGF plays its role through VEGF receptors (VEGFR) (Zhu & Zhou, 2015). VEGFR-2 is the primary VEGF receptor in humans, primarily expressed in endothelial cells, lymphatic endothelial cells, as well as in neurons, megakaryocytes, hematopoietic stem cells, and various types of cancer cells (Yang et al., 2018). Vascular endothelial growth factor receptor (VEGFR), particularly VEGFR-2, has been recognized as a prominent therapeutic target among receptor tyrosine kinases (Modi & Kulkarni, 2019). Recent studies have demonstrated that VEGFR-2 inhibitors not only enhance therapeutic efficacy but also inhibit tumor growth resistant to selective estrogen receptor modulators (SERMs) (Luo et al., 2017).

VEGFR-2 consists of an extracellular region comprising seven immunoglobulin-like domains, a transmembrane domain, and an intracellular region containing two tyrosine kinase domains (Shah et al., 2025). Activation of the VEGFR-2 signaling pathway plays a pivotal role in transduction cascades that initiate angiogenesis in pre-existing blood vessels, leading to the formation of new vasculature. Dysregulated angiogenesis may contribute to tumor growth and significantly increase the risk of cancer progression. Inhibition of VEGFR-2 can effectively suppress the angiogenic process (Luo et al., 2017; Yang et al., 2018). According to Yan et al. (2015), VEGFR-2 expression can be observed during the epithelial–mesenchymal transition (EMT), in which high levels of Twist1 and vimentin are associated with elevated VEGFR-2 expression. This finding indicates that EMT serves as a mediator of VEGFR-2.

The current breast cancer treatment modalities in Indonesia include chemotherapy, radiotherapy, and surgical intervention (Yan et al., 2015). However, these therapeutic approaches are often associated with substantial adverse effects. Furthermore, the financial burden of treatment remains relatively high. To minimize the potential adverse effects associated with current therapies, herbal medicines may serve as an alternative approach. Herbal remedies have gained increasing public interest due to their traditional use across generations and their reported therapeutic activities. Moreover, they are generally considered to possess lower toxicity compared to synthetic drugs. Nevertheless, further investigations are required to comprehensively characterize their pharmacological properties and therapeutic potential against specific diseases.

One medicinal plant that has attracted considerable attention for its pharmacological activities is the rhizome of *Kaempferia galanga* L. According to Yao et al. (2018), seventeen compounds have been isolated from the rhizome, including seven phenolics, six diarylheptanoids, one phenolic glycoside, one cyclic lipopeptide, and two esters. Galangal rhizome has been reported to exhibit antimicrobial, antioxidant, anti-inflammatory, analgesic, anti-tuberculosis, antithrombotic, anti-angiogenic, and anticancer effects (Swapana et al., 2018). Several studies have shown that p-methoxycinnamic acid and ethyl p-methoxycinnamate from galangal rhizomes display strong anticancer activity against various cancer cell lines (Kumar, 2020), and rhizome extracts suppress VEGF and COX-2 expression in the chorioallantoic membrane model (Hamid et al., 2019; Huang et al., 2024).

To date, the anti-angiogenic activity of K. galanga has been demonstrated only for whole extracts or a small number of cinnamate derivatives, and described phenomenologically: VEGF and COX-2 expression fall, and endothelial tube formation is reduced. Which individual constituents are responsible, and whether any of them act directly on VEGFR-2 rather than upstream of it, has not been determined. No study has yet evaluated the rhizome's phenolic and diterpenoid constituents against the VEGFR-2

kinase domain, so no structure-activity rationale explains why the rhizome is anti-angiogenic. An *in silico* approach was chosen to address this gap. Computational screening resolves this by evaluating each constituent individually and by reporting the binding mode rather than only the outcome, so that the residues engaged by each compound can be compared directly with those engaged by a validated VEGFR-2 inhibitor. Combining four complementary filters (Lipinski's Rule of Five, ADMET prediction, ligand-based pharmacophore screening, and molecular docking) further allows candidates to be ranked on drug-likeness and predicted safety as well as on affinity, which narrows the list before laboratory work is committed. Accordingly, ten compounds reported from the rhizome of *K. galanga* were evaluated in silico for their potential to inhibit VEGFR-2 in breast cancer.

Methods

Physicochemical Property Prediction

The prediction of the physicochemical properties of compounds in *Kaempferia galanga* rhizomes was carried out following the Lipinski Rule of Five (RO5). The analysis was performed using a personal laptop with the following specifications: Intel Core i5-10210U CPU @ 1.60 GHz, 2.11 GHz, 8.00 GB RAM, running the Windows 11 64-bit operating system on an x64-based processor. The analysis was performed using ten active compounds, namely vanillic acid, ferulic acid, methyl 3,4-dihydroxybenzoate, p-methoxybenzoic acid, p-hydroxybenzoic acid, methyl (2R,3S)-2,3-dihydroxy-3-(4-methoxyphenyl)propanoate, p-hydroxycinnamic acid, ethyl (2R,3S)-2,3-dihydroxy-3-(4-methoxyphenyl)propanoate, sandaracopimaradien-6β,9α-diol-1-one, and 4-methoxycinnamic acid derived from the rhizome of *Kaempferia galanga* using the Mcule platform (*https://mcule.com/*).

Prediction of ADME and Toxicity Profiles

The ten compounds that were tested and analyzed for their physicochemical properties were subsequently evaluated for ADME (Absorption, Distribution, Metabolism, and Excretion) and toxicity profiles using PreADMET (Incheon, South Korea; *https://preadmet.webservice.bmdrc.org/*). In this in silico study, the ADME parameters analyzed included human intestinal absorption (HIA), Caco-2 permeability, plasma protein binding (PPB), and blood–brain barrier (BBB) penetration, while the toxicity parameters included mutagenicity and carcinogenicity. The compound structures were drawn using the features provided on the online platform and subsequently submitted, after which the generated data were analyzed.

Pharmacophore Screening

Pharmacophore modeling was performed to identify hit compounds capable of exerting pharmacological activity through the presence of pharmacophoric groups. On the DUDE online platform (San Francisco, USA; *https://dude.docking.org/targets*), this process was applied to expand the list of active compounds by generating an Active/Decoy Database. The target protein used was VEGFR2, a vascular endothelial growth factor receptor 2, with PDB ID 2P2I. In the LigandScout application (Vienna, Austria) all active and decoy types were changed to training, while all test compounds were set to "Test", and the other fields were left blank. Once these modifications were made, one training type was obtained for each cluster after opening the minimized active database file. The process was then followed by the pharmacophore model formation. The model was therefore derived from the ligand set rather than from a single receptor structure, while the docking stage used the co-crystallised VEGFR-2 structure 3VO3 described below; the two stages probe complementary aspects of molecular recognition rather than duplicating each other.

A total of 10 pharmacophore models were transferred and validated using the "copy to other perspective" feature to the screening perspective. Active compounds were highlighted in green, and decoys were marked in red, resulting in the best ROC curve. The pharmacophore screening continued by transferring the database of test compounds into another database. Additionally, green coloring was applied to the test compound database, and any markers on the other databases were removed. The best model was then transferred to the screening perspective,

followed by performance screening to identify the hit compounds.

Molecular Docking

The research process began by downloading the protein corresponding to the target receptor from the Protein Data Bank (New Brunswick, USA; *https://www.rcsb.org/*), using the VEGFR-2 protein database with PDB ID code 3VO3 in pdb file format. Re-docking was then performed using BIOVIA Discovery Studio (San Diego, USA), along with AutoDock Tools-1.5.6 (La Jolla, USA) to validate the device, resulting in the native ligand imidazo[1,2-b]pyridazine derivative and the VEGFR2 receptor. The re-docking yielded an RMSD of 1.29 Å, with the grid box coordinates set at X = 40; Y = 40; Z = 40, and the grid coordinates X = 4.638; Y = -26.834; Z = -31.463, with a spacing of 0.375 Å. This was followed by the docking process of the VEGFR2 receptor with the test compounds (Ismail et al., 2025).

Result and Discussion

Galangal rhizomes (*Kaempferia galanga* L.) are widely recognized by the public as a culinary spice and are also known for their health benefits. Numerous studies have investigated galangal for its anticancer and antiangiogenic properties, particularly in breast cancer, using in silico, in vitro, and in vivo approaches that involve various receptors. These studies have demonstrated that several compounds from galangal exhibit promising anticancer and antiangiogenic activities and could serve as potential candidates for the development of new breast cancer therapies. Research also indicates that isolates of p-methoxycinnamic acid and ethyl p-methoxycinnamate from galangal rhizomes exhibit potent anticancer activity against various cancer cell lines (Kalontong et al., 2022; Kumar, 2020).

The antiangiogenic mechanism of galangal involves inhibiting the growth and spread of cancer cells by blocking the formation of new blood vessels. Other antiangiogenic effects include the inhibition of endothelial cell activity such as proliferation, migration, and tube formation, and the suppression of pro-angiogenic factor expression, particularly VEGF and COX-2 (Hamid et al., 2019; Huang et al., 2024). Despite the presence of many active compounds in galangal rhizomes, these findings are still in the preclinical research phase and require further clinical studies to better evaluate the potential of *K. galanga* as a complementary therapy for breast cancer. Identifying which individual constituents are responsible for this activity, and on which molecular target they act, is therefore a necessary step before any clinical evaluation can be designed.

Pharmacophore modeling and docking are essential methods in the drug discovery process. Pharmacophore modeling allows us to identify the structural similarities between test compounds and known active compounds. Docking, on the other hand, helps us understand how the test compounds interact with receptors, providing clearer insights into how well the test compounds can bind to molecular targets and their potential as drugs (Yasmin & Beloshe, 2025). Therefore, the pharmacophore procedure we carried out involved applying Lipinski's rule of five prediction, determining ADMET properties, performing pharmacophore screening, and conducting molecular docking.

Lipinski's Rule of Five (RO5) Prediction

Lipinski's Rule of Five (RO5) is a widely used guideline in drug discovery that predicts the likelihood of a compound being orally active in humans. According to this rule, good oral bioavailability is expected if the compound does not violate more than one of the following criteria: molecular weight ≤ 500 Da, LogP ≤ 5, fewer than five hydrogen bond donors, and fewer than 10 hydrogen bond acceptors (Lipinski et al., 2001). Based on the results of the tests summarized in Table 1, in accordance with the predictions of Lipinski's Rule of Five, it can be concluded that 10 compounds from the rhizomes of *Kaempferia galanga* L. meet the criteria of Lipinski's Rule of Five (RO5). Therefore, these compounds have the potential to be considered as candidates for further development as oral-administrated drugs.

Table 1. Results of Lipinski's Rule of Five (RO5) Prediction

Compound Name	Molecular Weight (< 500 Da) 1 Da = 1 g/mol)	Log P (<5)	Hydrogen Bonds		Remark
			Donor (<5)	Acceptor (< 10)	
Vanillic acid	168.15	1.40	2	4	Pass
Ferulic acid	194.18	1.50	2	4	Pass
Methyl 3,4-dihidroxybenzoate	168.15	1.48	2	4	Pass
p-Methoxybenzoicacid	152.14	1.39	1	3	Pass
p-Hydroxybenzoicacid	138.12	1.09	2	3	Pass
Methyl(2R,3S)-2,3-dihydroxy-3-(4-methoxyphenyl)propanoate	226.22	0.26	2	5	Pass
p-Hydroxycinnamic acid	164.15	1.49	2	3	Pass
Ethyl (2R,3S)-2,3-dihydroxy-3-(4-methoxyphenyl) propanoate	240.25	0.65	2	5	Pass
Sandaracopimaradien-6β,9α-diol-1-one	302.45	4.29	1	2	Pass
4-Methoxycinnamic acid	178.18	1.79	1	3	Pass

Determination of ADMET

ADMET (absorption, distribution, metabolism, excretion and toxicity) prediction is a crucial step in evaluating drug-likeness, because it anticipates the pharmacokinetic behaviour and safety of candidate compounds before isolation or synthesis is attempted (Koutroumpa et al., 2025; Li, 2001). The profiling was performed on the compounds that complied with Lipinski's Rule of Five and is presented in Table 2. Each parameter is interpreted below in terms of what it means for an orally administered anti-angiogenic candidate.

Human intestinal absorption (HIA) predicts the percentage of an oral dose crossing the intestinal epithelium, with values above 70% classed as well absorbed and below 20% as poorly absorbed. All ten compounds fell in the well-absorbed class, ranging from 84.94% for methyl 3,4-dihydroxybenzoate to 100.00% for sandaracopimaradien-6β,9α-diol-1-one. None would therefore be lost to poor oral uptake, but because the whole set clusters at the top of the scale, HIA does not discriminate between the candidates.

Caco-2 permeability models transport across the intestinal monolayer, with values above 70 nm/s classed as high, 4–70 nm/s as moderate and below 4 nm/s as low. None of the ten compounds exceeded 70 nm/s. The values clustered narrowly between 19.93 and 23.41 nm/s, which places every compound in the moderate class rather than the high-permeability class. Intestinal transport is therefore adequate but not outstanding, and formulation strategies that enhance permeability may be worth considering should any of these compounds progress.

Plasma protein binding (PPB) determines how much drug remains free and pharmacologically active, with values above 90% indicating strong binding and a correspondingly small free fraction. Only sandaracopimaradien-6β,9α-diol-1-one was strongly bound (100.00%). The remaining nine compounds bound weakly, from 8.04% for p-hydroxybenzoic acid to 76.02% for 4-methoxycinnamic acid, leaving a larger free fraction available to reach the tumour vasculature. For an agent intended to act on endothelial VEGFR-2, this is favourable, and it counts against the diterpenoid.

Blood–brain barrier (BBB) penetration is reported as the brain-to-blood concentration ratio: values above 2.0 indicate ready entry into the central nervous system, 0.1–2.0 moderate entry and below 0.1 little or none (Xiong et al., 2021). Low CNS exposure is preferable for a peripherally acting anti-angiogenic agent because it limits neurological side effects. Eight compounds showed moderate penetration (0.40–1.74), ethyl (2R,3S)-2,3-dihydroxy-3-(4-methoxyphenyl)propanoate gave the lowest value at 0.06, and sandaracopimaradien-6β,9α-diol-1-one was a clear outlier at 16.13, predicting substantial CNS exposure and an associated risk of central effects.

Table 2. Results of ADMET Determination

Compound Name	Absorption		Distribution			Toxicity	
	HIA (%)	Caco-2 (nm/sec)	PPB (%)	BBB	Mutagen	Carcinogen	
						Rat	Mouse
Vanillic acid	85.36	19.93	52.10	0.62	Mutagen	Negative	Positive
Ferulic acid	90.60	21.11	50.41	0.75	Mutagen	Negative	Positive
Methyl 3,4-dihidroxybenzoate	84.94	19.93	72.28	0.50	Mutagen	Negative	Positive
p-Methoxybenzoicacid	94.33	20.79	45.90	1.35	Mutagen	Negative	Negative
p-Hydroxybenzoicacid	88.13	20.31	8.04	0.64	Mutagen	Negative	Negative
Methyl(2R,3S)-2,3-dihydroxy-3-(4-methoxyphenyl)propanoate	86.16	21.25	37.18	0.40	Mutagen	Negative	Negative
p-Hydroxycinnamic acid	92.09	21.10*	63.05	0.69	Mutagen	Negative	Positive
Ethyl (2R,3S)-2,3-dihydroxy-3-(4-methoxyphenyl) propanoate	87.56	21.81	44.05	0.06	Mutagen	Negative	Negative
Sandaracopimaradien-6β,9α-diol-1-one	100.00	23.41*	100.00	16.13	Mutagen	Negative	Positive
4-Methoxycinnamic acid	96.72	21.42	76.02	1.74	Mutagen	Positive	Positive

The toxicity predictions were the most restrictive filter. All ten compounds were predicted mutagenic in the Ames model, which reflects the phenolic and α,β-unsaturated carbonyl motifs common to this compound class; this is a general caution rather than a discriminating result, and experimental Ames testing will be required before any of these compounds is taken further. Carcinogenicity prediction separated the set more usefully. Four compounds were predicted non-carcinogenic in both rat and mouse: p-methoxybenzoic acid, p-hydroxybenzoic acid, methyl (2R,3S)-2,3-dihydroxy-3-(4-methoxyphenyl) propanoate and ethyl (2R,3S)-2,3-dihydroxy-3-(4-methoxyphenyl) propanoate. Five were negative in rat but positive in mouse, and 4-methoxycinnamic acid was positive in both species, which makes it the least attractive candidate on safety grounds despite its favourable pharmacophore fit.

Taken together, the ADMET profile favours the two propanoate esters and the two benzoic acids: all four are well absorbed, moderately permeable, weakly protein-bound, predicted to have limited CNS exposure and non-carcinogenic in both rodent species. Sandaracopimaradien-6β,9α-diol-1-one is the least favourable compound on this evidence, combining complete plasma protein binding with high predicted BBB penetration and predicted carcinogenicity in mouse.

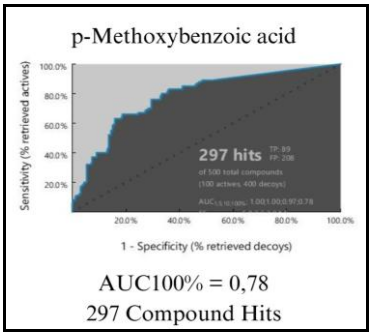


Figure 1. ROC Curve of Model 4 from Pharmacophore Screening

Pharmacophore Screening

Pharmacophore screening is a ligand-based drug discovery technique that identifies the essential three-dimensional structural features responsible for biological activity in known active compounds. By constructing and validating pharmacophore models, researchers can efficiently distinguish active from inactive molecules and perform virtual screening of large compound libraries to identify potential drug candidates (Pal et al., 2019). A model with a ROC curve AUC value greater than 0.7 is considered capable of distinguishing active from inactive compounds (Wolber & Langer, 2005). Among the ten ROC curve models constructed, Model 4 was selected as the optimal model because it had an AUC value of 0.78, indicating good discriminatory ability by this criterion. Model 4 retrieved 297 hits from the 500-compound validation set, comprising 89 of the 100 known actives and 208 of the 400 decoys, and its early enrichment was high, with AUC values of 1.00, 1.00 and 0.97 at the 1%, 5% and 10% cut-offs respectively (Figure 1). The model therefore ranks true actives at the top of the list even though it retrieves a substantial number of decoys overall.

Of the ten test compounds, eight mapped onto Model 4 and were retrieved as hits; p-hydroxybenzoic acid and sandaracopimaradien-6β,9α-diol-1-one were not. p-Hydroxybenzoic acid is the smallest member of the set and cannot span the distance between the model's hydrogen-bonding features, whereas sandaracopimaradien-6β,9α-diol-1-one is a hydrophobic diterpenoid that lacks the donor and acceptor groups the model requires. Both exclusions are therefore consistent with the chemistry of the model rather than artefacts. The compound that showed the best interaction was Methyl(2R,3S)-2,3-dihydroxy-3-(4-methoxyphenyl)propanoate, with a fit score of 38.35%. These results indicate that the eight compounds exhibit activity and interact with the VEGFR2 receptor. Therefore, it is expected that these 8 test compounds may exhibit significant anti-breast cancer activity and thus serve as candidates for the development of herbal medicines as complementary therapies in breast cancer treatment, as presented in Table 3.

Table 3. Hit Compound Screening Results

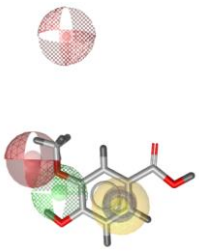
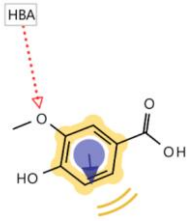
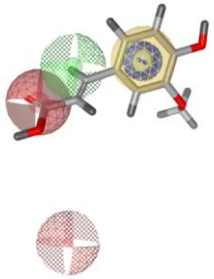
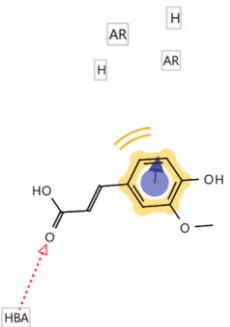
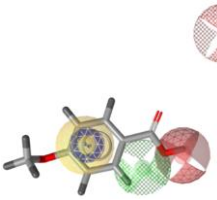
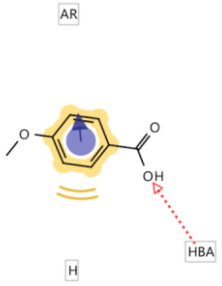
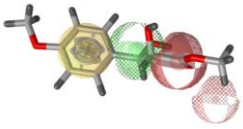
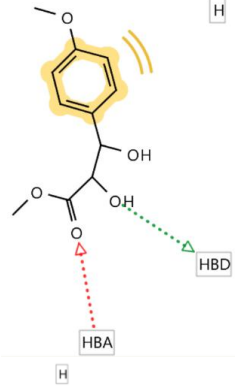
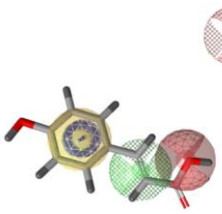
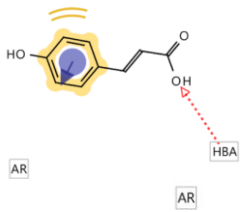
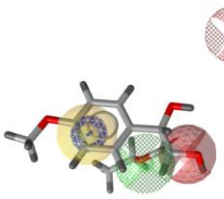
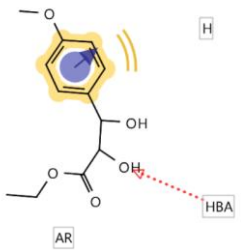
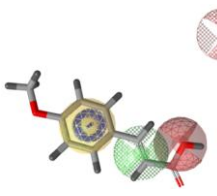
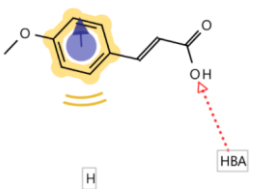
Compound	3D Result	2D Result	Fit Score
Vanillic acid			35.28
Ferulic acid			38.01

Table 3. Continued

Compound	3D Result	2D Result	Fit Score
Methyl 3,4-dihidroxybenzoate			36.35
Methyl(2R,3S)-2,3-dihydroxy-3-(4-methoxyphenyl)propanoate			38.35
p-Hydroxycinnamic acid			38.05
Ethyl (2R,3S)-2,3-dihydroxy-3-(4-methoxyphenyl) propanoate			36.25
4-Methoxycinnamic acid			38.07

Molecular Docking

The validity of the docking protocol was assessed from the RMSD of the redocked native ligand, which measures the deviation between the redocked pose and the crystallographic pose and is regarded as acceptable at ≤ 2.0 Å. A low RMSD indicates that the protocol reproduces the experimentally observed binding mode. The validation parameters are collected in Table 4. Binding energy (ΔG) and the inhibition constant (Ki) are not independent quantities: they are linked by $\Delta G = RT \ln Ki$, where R is the gas constant and T the absolute temperature. A more

negative ΔG therefore corresponds to an exponentially smaller Ki, and the two parameters always rank compounds in the same order; Ki simply restates the same affinity on a concentration scale, as the predicted concentration at which half of the receptor is occupied (Forli et al., 2016; Sangande et al., 2020). The complete docking results are summarised in Table 5.

Table 4. Validation of the molecular docking protocol by redocking of the native ligand

Validation parameter	Value
Receptor	VEGFR-2 (PDB ID: 3VO3)
Native ligand	Imidazo[1,2-b]pyridazine derivative
RMSD (Å)	1.29
Binding energy (kcal/mol)	-10.81
Inhibition constant, Ki	11.93 nM
Grid box size	40 × 40 × 40 points, spacing 0.375 Å
Grid centre (x, y, z)	4.638, -26.834, -31.463

Table 5. Molecular Docking Result

Compound	*Binding energy (kcal/mol)*	Ki	Interaction with Amino Acids	
			Hydrogen Bonds	Other Interactions
Imidazo[1,2-b]pyridazine	-10.81	11.93 nM	Leu A: 840 Glu A: 885 Cys A: 1045	Alkyl & Pi-Alkyl: Val A: 848, Phe A: 918, Leu A: 1035, Ala A: 866, Val A: 899, Leu A: 1019, Val A: 898, His A: 1026 Pi-Sigma: Val A: 916 Pi-Sulfur: Lys A: 868, Cys A: 919.
Vanillic acid	-6.04	37.25 µM	Lys A: 868 Glu A: 885 Cys A: 919	Alkyl & Pi-Alkyl : Ala A: 866, Leu A: 1035,Val A: 848, Val A: 899, Phe A: 918, Leu A: 840
Ferulic acid	-6.04	37.21 µM	Lys A: 868 Glu A: 885 Cys A: 919	Alkyl & Pi-Alkyl : Ala A: 866, Leu A: 1035,Val A: 848, Val A: 899, Phe A: 918, Leu A: 840
Methyl 3,4-dihidroxybenzoate	-6.05	37.03 µM	Lys A: 868 Glu A: 885 Cys A: 919	Alkyl & Pi-Alkyl : Ala A: 866, Leu A: 1035,Val A: 848, Val A: 899, Leu A: 840, Phe A: 918
p-Methoxybenzoicacid	-6.04	37.65 µM	Asp A: 1046 Cys A: 919	Alkyl & Pi-Alkyl : Val A: 899, Phe A: 918, Leu A: 840, Val A: 848, Ala A: 866, Leu A: 1035
p-Hydroxybenzoicacid	-6.04	37.33 µM	Asp A: 1046 Cys A: 919	Alkyl & Pi-Alkyl : Ala A: 866, Val A: 848, Leu A: 840, Phe A: 918, Leu A: 1035

Table 5. Continued

Compound	*Binding energy (kcal/mol)*	Ki	Interaction with Amino Acids	
			Hydrogen Bonds	**Other Interactions**
Methyl(2R,3S)-2,3-dihydroxy-3-(4-methoxyphenyl)propanoate	-6.04	37.43 µM	Lys A: 868 Glu A: 885 Cys A: 919	Alkyl & Pi-Alkyl : Ala A: 866, Leu A: 1035,Val A: 848, Val A: 899, Leu A: 840, Phe A: 918
p-Hydroxycinnamic acid	-6.04	37.61 µM	Lys A: 868 Glu A: 885 Cys A: 919	Alkyl & Pi-Alkyl : Ala A: 866, Leu A: 1035,Val A: 848, Val A: 899, Leu A: 840, Phe A: 918
Ethyl (2R,3S)-2,3-dihydroxy-3-(4-methoxyphenyl) propanoate	-6.04	37.42 µM	Cys A: 919 Glu A: 885 Lys A: 868	Alkyl & Pi-Alkyl : Phe A: 918 Ala A: 866, Leu A: 840, Val A: 899, Val A: 848, Leu A: 1035
Sandaracopimaradien-6β,9α-diol-1-one	-9.23	172.53 nM	-	Alkyl & Pi-Alkyl : Cys A: 919, Leu A: 840, Phe A: 918, Phe A: 1047, Ala A: 866, Val A: 848, Val A: 899, Val A: 916, Lys A: 868, Val A: 914, Cys A: 1045, Leu A: 1035
4-Methoxycinnamic acid	-6.04	37.53 µM	Lys A: 868 Glu A: 885 Cys A: 919	Alkyl & Pi-Alkyl : Ala A: 866, Val A: 848, Val A: 899, Phe A: 918, Leu A: 840, Leu A: 1035

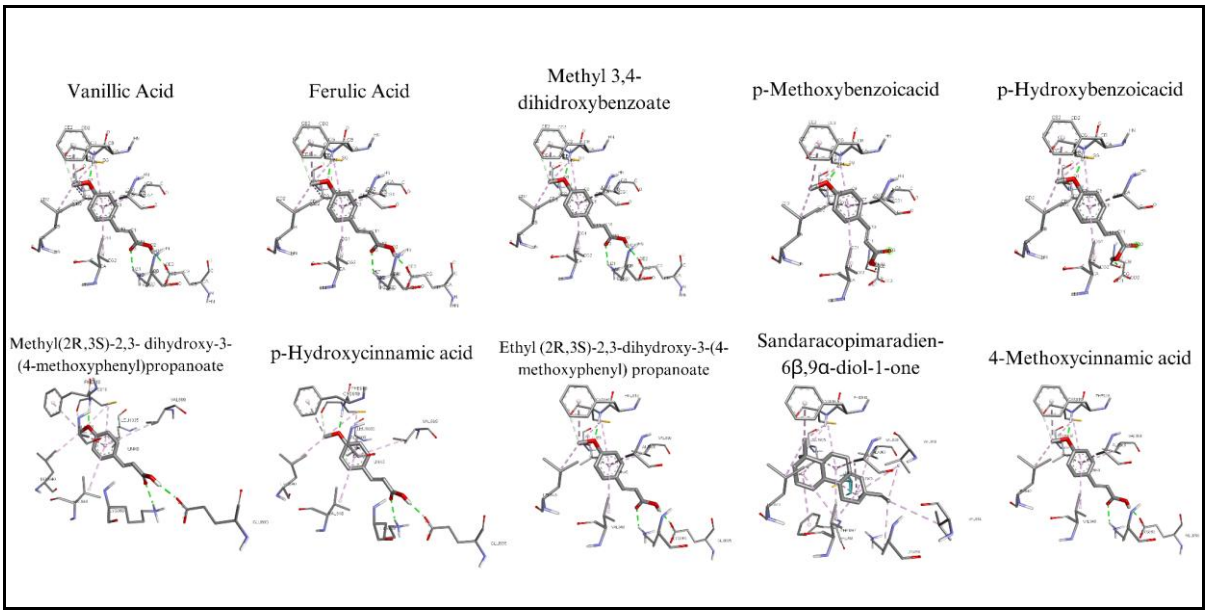


Figure 2. Visualization of Molecular Docking Simulation of Test Compounds

Validation was performed by re-docking the VEGFR2 receptor (PDB ID: 3VO3) with its native ligand, an Imidazo[1,2-b]pyridazine derivative known to inhibit VEGFR2 tyrosine kinase activity. The re-docking produced an RMSD of 1.29 Å, a binding energy of -10.81 kcal/mol, and an inhibition constant of 11.93 nM, confirming the validity of the molecular docking protocol. Validation is a crucial step in molecular docking studies to ensure the accuracy of binding predictions (Nursanti et al., 2022).

Applying that relationship to the present data, the native imidazo[1,2-b]pyridazine ligand bound most strongly (ΔG = -10.81 kcal/mol; Ki = 11.93 nM). Among the test compounds, sandaracopimaradien-6β,9α-diol-1-one was the only one to approach it (-9.23 kcal/mol; Ki = 172.53 nM), roughly fourteen times weaker than the native ligand. The eight phenolic compounds formed a tight cluster between -6.04 and -6.05 kcal/mol, with Ki values of 37.03–37.65 μM, about three orders of magnitude weaker than the native ligand. The near-identical scores within this cluster reflect their close structural similarity, since all are small benzoic or cinnamic acid derivatives of comparable size and polarity occupying the same pocket. Docking energy alone therefore cannot rank them, and discrimination has to come from the pharmacophore fit and the ADMET profile.

The interactions themselves account for these differences. The native ligand is anchored by three hydrogen bonds to Leu840 and Glu885 in the hinge and gatekeeper region and to Cys1045 in the DFG motif, supported by an extensive alkyl and pi-alkyl network with Val848, Ala866, Leu1035, Val899, Phe918 and Leu1019, a pi-sigma contact with Val916 and pi-sulfur contacts with Lys868 and Cys919. Hydrogen bonding to Glu885 and Cys1045 is characteristic of type II VEGFR-2 inhibition, because it locks the kinase in the inactive DFG-out conformation and prevents ATP binding. The functional consequence is loss of receptor autophosphorylation and suppression of the downstream PLC-gamma/ERK and PI3K/AKT cascades that drive endothelial proliferation, migration and tube formation, which is the molecular basis of the anti-angiogenic effect sought here.

Seven test compounds, namely vanillic acid, ferulic acid, methyl 3,4-dihydroxybenzoate, methyl (2R,3S)-2,3-dihydroxy-3-(4-methoxyphenyl)propanoate, p-hydroxycinnamic acid, ethyl (2R,3S)-2,3-dihydroxy-3-(4-methoxyphenyl)propanoate and 4-methoxycinnamic acid, reproduced part of this pattern. Each formed hydrogen bonds with Lys868, Glu885 and Cys919 together with alkyl and pi-alkyl contacts to Ala866, Val848, Val899, Leu840, Phe918 and Leu1035. Retention of the Glu885 hydrogen bond matters, because this is the residue through which the native ligand stabilises the inactive conformation; it indicates that these compounds occupy the same pocket and could in principle act by the same mechanism, although at much lower affinity. p-Methoxybenzoic acid and p-hydroxybenzoic acid instead hydrogen-bonded to Asp1046 and Cys919 without engaging Glu885, so their binding mode diverges from that of the native ligand. Sandaracopimaradien-6β,9α-diol-1-one formed no hydrogen bonds at all; its low binding energy derives entirely from twelve alkyl and pi-alkyl contacts. Purely hydrophobic binding of this kind is less specific and more readily displaced than a hydrogen-bonded complex, which is an important qualification on its apparent potency.

These observations resolve the apparent contradiction between the two screening stages. Sandaracopimaradien-6β,9α-diol-1-one ranked first in docking yet was not retrieved by the pharmacophore model, and it was excluded for a consistent reason rather than by error: the model encodes the hydrogen-bond donor and acceptor features shared by known VEGFR-2 actives, and a diterpenoid that binds purely through hydrophobic contact possesses none of them. The two methods are not in conflict; they measure different properties, and this compound satisfies one criterion while failing the other. Its ADMET profile reinforces the point, since it was the only compound combining complete plasma protein binding with high predicted BBB penetration.

Judged on all four filters together rather than on docking score alone, methyl (2R,3S)-2,3-dihydroxy-3-(4-methoxyphenyl)propanoate is the most promising candidate from K. galanga. It satisfies all four Lipinski criteria; it was predicted non-carcinogenic in both rat and

mouse, one of only four compounds in that category; it is weakly protein-bound (37.18%) with low predicted CNS exposure (BBB 0.40); it obtained the highest pharmacophore fit score of the hit set (38.35); and it reproduces the native ligand's hydrogen bond to Glu885 within the same binding pocket. No other compound meets all five conditions. Ferulic acid, p-hydroxycinnamic acid and 4-methoxycinnamic acid have comparable fit scores but each is predicted carcinogenic in at least one rodent species, and sandaracopimaradien-6β,9α-diol-1-one, despite the lowest binding energy, fails both the pharmacophore filter and the safety filter.

The in silico findings suggest that compounds from galangal rhizomes possess promising potential as anticancer agents and VEGFR2 inhibitors. Nevertheless, further validation through in vitro and in vivo studies is essential to confirm their efficacy, establish their safety profiles, and evaluate their prospects for therapeutic development.

Conclusion

Taking drug-likeness, predicted toxicity, pharmacophore fit, and binding mode together, methyl (2R,3S)-2,3-dihydroxy-3-(4-methoxyphenyl)propanoate emerges as the lead candidate, supported by four parameters: no Lipinski violation, predicted non-carcinogenicity in both rodent species, the highest pharmacophore fit score of the hit set (38.35), and retention of the Glu885 hydrogen bond. Sandaracopimaradien-6β,9α-diol-1-one gave the lowest binding energy (-9.23 kcal/mol) but binds only through hydrophobic contacts and was unfavourable in plasma protein binding, BBB penetration, and pharmacophore fit, so it is not recommended as a lead.

Two limitations bound these conclusions: all ten compounds were predicted mutagenic in the Ames model, and the affinities of the phenolic compounds remain three orders of magnitude below that of the native ligand. The immediate prospects are therefore threefold. First, molecular dynamics simulation should test whether the Glu885 hydrogen bond in the lead compound persists over time. Second, in vitro confirmation by VEGFR-2 kinase inhibition and endothelial tube-formation assays is needed, with experimental Ames testing alongside. Third, structural modification of the propanoate scaffold should be explored to raise affinity, since the present results identify the dihydroxy-propanoate arm reaching Glu885 as the feature to preserve during optimisation.

References

Forli, S., Huey, R., Pique, M. E., Sanner, M. F., Goodsell, D. S., & Olson, A. J. (2016). Computational protein–ligand docking and virtual drug screening with the AutoDock suite. *Nature Protocols*, *11*(5), 905–919. https://doi.org/10.1038/nprot.2016.051

Ghoncheh, M., Pournamdar, Z., & Salehiniya, H. (2016). Incidence and Mortality and Epidemiology of Breast Cancer in the World. *Asian Pacific Journal of Cancer Prevention: APJCP*, *17*(S3), 43–46. https://doi.org/10.7314/apjcp.2016.17.s3.43

Hamid, I. S., Ekowati, J., & Purnama, M. T. E. (2019). Kaempferia galanga L. Inhibiting Effect on Vascular Endothelial Growth Factor (VEGF) and Cyclooxygenase-2 (Cox-2) Expression on Endothelium of Chorioallantoic Membrane. *Indian Veterinary Journal*, *96*(9), 80–82.

Huang, W., Zheng, N., Niu, N., Tan, Y., Li, Y., & Tian, H. (2024). Potent anti-angiogenic component in *Kaempferia galanga* L. and its mechanism of action. *Journal of Ethnopharmacology*, *324*, 117811. https://doi.org/10.1016/j.jep.2024.117811

Ismail, D. P. F., Christella, A., Salsabila, N. F., Angelina, A., Muljono, F. O., Fardhan, F. M., & Novitasari, D. (2025). The bioactive compounds in bilimbi leaves (Averrhoa bilimbi L.) as natural-based anticancer targeting on VEGFR-2: In silico studies. *Notulae Scientia Biologicae*, *17*(1), 12289–12289. https://doi.org/10.55779/nsb17112289

Kalontong, P. K., Safithri, M., & Tarman, K. (2022). Molecular Docking of Active Compound of Spirulina platensis as TMPRSS2 Inhibitor to Prevent the SARS-COV-2 Infection. *Jurnal Pengolahan Hasil Perikanan Indonesia*, *25*(2), 253–267.

Koutroumpa, N.-M., Tsoumanis, A., Sarimveis, H., Lynch, I., Melagraki, G., & Afantitis, A.

(2025). Prediction of blood–brain barrier and Caco-2 permeability through the Enalos Cloud Platform: Combining contrastive learning and atom-attention message passing neural networks. *Journal of Cheminformatics*, *17*(1), 68. https://doi.org/10.1186/s13321-025-01007-2

Kumar, A. (2020). Phytochemistry, pharmacological activities and uses of traditional medicinal plant *Kaempferia galanga* L. – An overview. *Journal of Ethnopharmacology*, *253*, 112667. https://doi.org/10.1016/j.jep.2020.112667

Li, A. P. (2001). Screening for human ADME/Tox drug properties in drug discovery. *Drug Discovery Today*, *6*(7), 357–366. https://doi.org/10.1016/S1359-6446(01)01712-3

Lipinski, C. A., Lombardo, F., Dominy, B. W., & Feeney, P. J. (2001). Experimental and computational approaches to estimate solubility and permeability in drug discovery and development settings. *Advanced Drug Delivery Reviews*, *46*(1–3), 3–26. https://doi.org/10.1016/s0169-409x(00)00129-0

López-Camacho, E., García-Godoy, M. J., García-Nieto, J., Nebro, A. J., & Aldana-Montes, J. F. (2016). A New Multi-objective Approach for Molecular Docking Based on RMSD and Binding Energy. In M. Botón-Fernández, C. Martín-Vide, S. Santander-Jiménez, & M. A. Vega-Rodríguez (Eds.), *Algorithms for Computational Biology* (pp. 65–77). Springer International Publishing. https://doi.org/10.1007/978-3-319-38827-4_6

Luo, G., Li, X., Zhang, G., Wu, C., Tang, Z., Liu, L., You, Q., & Xiang, H. (2017). Novel SERMs based on 3-aryl-4-aryloxy-2H-chromen-2-one skeleton—A possible way to dual ERα/VEGFR-2 ligands for treatment of breast cancer. *European Journal of Medicinal Chemistry*, *140*, 252–273. https://doi.org/10.1016/j.ejmech.2017.09.015

Mboi, N., Syailendrawati, R., Ostroff, S. M., Elyazar, I. R., Glenn, S. D., Rachmawati, T., Nugraheni, W. P., Ali, P. B., Trisnantoro, L., Adnani, Q. E. S., Agustiya, R. I., Laksono, A. D., Aji, B., Amalia, L., Ansariadi, A., Antriyandarti, E., Ardani, I., Ariningrum, R., Aryastami, N. K., … Mokdad, A. H. (2022). The state of health in Indonesia's provinces, 1990–2019: A systematic analysis for the Global Burden of Disease Study 2019. *The Lancet Global Health*, *10*(11), e1632–e1645. https://doi.org/10.1016/S2214-109X(22)00371-0

Modi, S. J., & Kulkarni, V. M. (2019). Vascular Endothelial Growth Factor Receptor (VEGFR-2)/KDR Inhibitors: Medicinal Chemistry Perspective. *Medicine in Drug Discovery*, *2*, 100009. https://doi.org/10.1016/j.medidd.2019.100009

Nursanti, O., Wardani, I., & Hadisoebroto, G. (2022). Validasi Penambatan Molekuler (Docking) (Zingiber Officinale) dan (Cymbopogon citratus) Sebagai Ligan Aktif Reseptor Pparγ. *Jurnal Farmasi Higea*, *14*(1), 79–94. https://doi.org/10.52689/higea.v14i1.469

Pal, S., Kumar, V., Kundu, B., Bhattacharya, D., Preethy, N., Reddy, M. P., & Talukdar, A. (2019). Ligand-based Pharmacophore Modeling, Virtual Screening and Molecular Docking Studies for Discovery of Potential Topoisomerase I Inhibitors. *Computational and Structural Biotechnology Journal*, *17*, 291–310. https://doi.org/10.1016/j.csbj.2019.02.006

Patel, S. A., Nilsson, M. B., Le, X., Cascone, T., Jain, R. K., & Heymach, J. V. (2023). Molecular Mechanisms and Future Implications of VEGF/VEGFR in Cancer Therapy. *Clinical Cancer Research*, *29*(1), 30–39. https://doi.org/10.1158/1078-0432.CCR-22-1366

Rizka, A., Akbar, M. K., & Putri, N. A. (2022). Carcinoma Mammae Sinistra T4bN2M1 Metastasis Pleura. *AVERROUS: Jurnal Kedokteran Dan Kesehatan Malikussaleh*, 23–31. https://doi.org/10.29103/averrous.v8i1.7006

Sangande, F., Julianti, E., & Tjahjono, D. H. (2020). Ligand-Based Pharmacophore Modeling, Molecular Docking, and Molecular Dynamic Studies of Dual Tyrosine Kinase Inhibitor of EGFR and VEGFR2. *International Journal of Molecular Sciences*, *21*(20), 7779. https://doi.org/10.3390/ijms21207779

Satriyo, A., Mutmainnah, E., Dewayani, M., & Dewi, D. S. (2018). Metastasis Kulit Tipe Karsinoma Erisipeloides Pada Pasien

Dengan Riwayat Kanker Payudara. *Media Dermato-Venereologica Indonesiana*, *45*(1). https://doi.org/10.33820/mdvi.v45i1.14

Shah, F. H., Nam, Y. S., Bang, J. Y., Hwang, I. S., Kim, D. H., Ki, M., & Lee, H.-W. (2025). Targeting vascular endothelial growth receptor-2 (VEGFR-2): Structural biology, functional insights, and therapeutic resistance. *Archives of Pharmacal Research*, *48*(5), 404–425. https://doi.org/10.1007/s12272-025-01545-1

Sung, H., Ferlay, J., Siegel, R. L., Laversanne, M., Soerjomataram, I., Jemal, A., & Bray, F. (2021). Global cancer statistics 2020: GLOBOCAN estimates of incidence and mortality worldwide for 36 cancers in 185 countries. CA: A Cancer Journal for Clinicians, 71(3), 209–249. https://doi.org/10.3322/caac.21660

Swapana, N., Tominaga, T., Elshamy, A. I., Ibrahim, M. A. A., Hegazy, M.-E. F., Brajakishor Singh, Ch., Suenaga, M., Imagawa, H., Noji, M., & Umeyama, A. (2018). Kaemgalangol A: Unusual seco-isopimarane diterpenoid from aromatic ginger *Kaempferia galanga*. *Fitoterapia*, *129*, 47–53. https://doi.org/10.1016/j.fitote.2018.06.010

Wolber, G., & Langer, T. (2005). LigandScout: 3-D pharmacophores derived from protein-bound ligands and their use as virtual screening filters. *Journal of Chemical Information and Modeling*, *45*(1), 160–169. https://doi.org/10.1021/ci049885e

Xiong, G., Wu, Z., Yi, J., Fu, L., Yang, Z., Hsieh, C., Yin, M., Zeng, X., Wu, C., Lu, A., Chen, X., Hou, T., & Cao, D. (2021). ADMETlab 2.0: An integrated online platform for accurate and comprehensive predictions of ADMET properties. *Nucleic Acids Research*, *49*(W1), W5–W14. https://doi.org/10.1093/nar/gkab255

Yan, Y., Zuo, X., & Wei, D. (2015). Concise Review: Emerging Role of CD44 in Cancer Stem Cells: A Promising Biomarker and Therapeutic Target. *Stem Cells Translational Medicine*, *4*(9), 1033–1043. https://doi.org/10.5966/sctm.2015-0048

Yang, J.-G., Wang, L.-L., & Ma, D.-C. (2018). Effects of vascular endothelial growth factors and their receptors on megakaryocytes and platelets and related diseases. *British Journal of Haematology*, *180*(3), 321–334. https://doi.org/10.1111/bjh.15000

Yao, F., Huang, Y., Wang, Y., & He, X. (2018). Anti-inflammatory diarylheptanoids and phenolics from the rhizomes of kencur (*Kaempferia galanga* L.). *Industrial Crops and Products*, *125*, 454–461. https://doi.org/10.1016/j.indcrop.2018.09.026

Yasmin, M., & Beloshe, V. (2025). Pharmacophore modeling in drug design. In *Advances in Pharmacology* (Vol. 103, pp. 313–324). Academic Press. https://doi.org/10.1016/bs.apha.2025.01.010

Zhu, X., & Zhou, W. (2015). The Emerging Regulation of VEGFR-2 in Triple-Negative Breast Cancer. *Frontiers in Endocrinology*, *6*. https://doi.org/10.3389/fendo.2015.00159